Machine Learning techniques applied to cosmological problems.

Martín de los Rios

Director: Dr. Mariano Domínguez

Resumen

Introduction to Machine Learning techniques.

The MeSsI (Merging Systems Identification) Algorithm.

Analysis of individual merging clusters candidates.
- A2029/2033.
- A1204.
- A267.
- Statistical analysis of the magnetic fields in merging clusters.

CosmoMl:Machine Learning techniques applied to the CMB.
- Construction of the data set.
- Unsupervised methods.
- Supervised methods.
- Cosmological parameters Angular distributions.

Conclusions.

Introduction to Machine Learning techniques.

Supervised Learning.

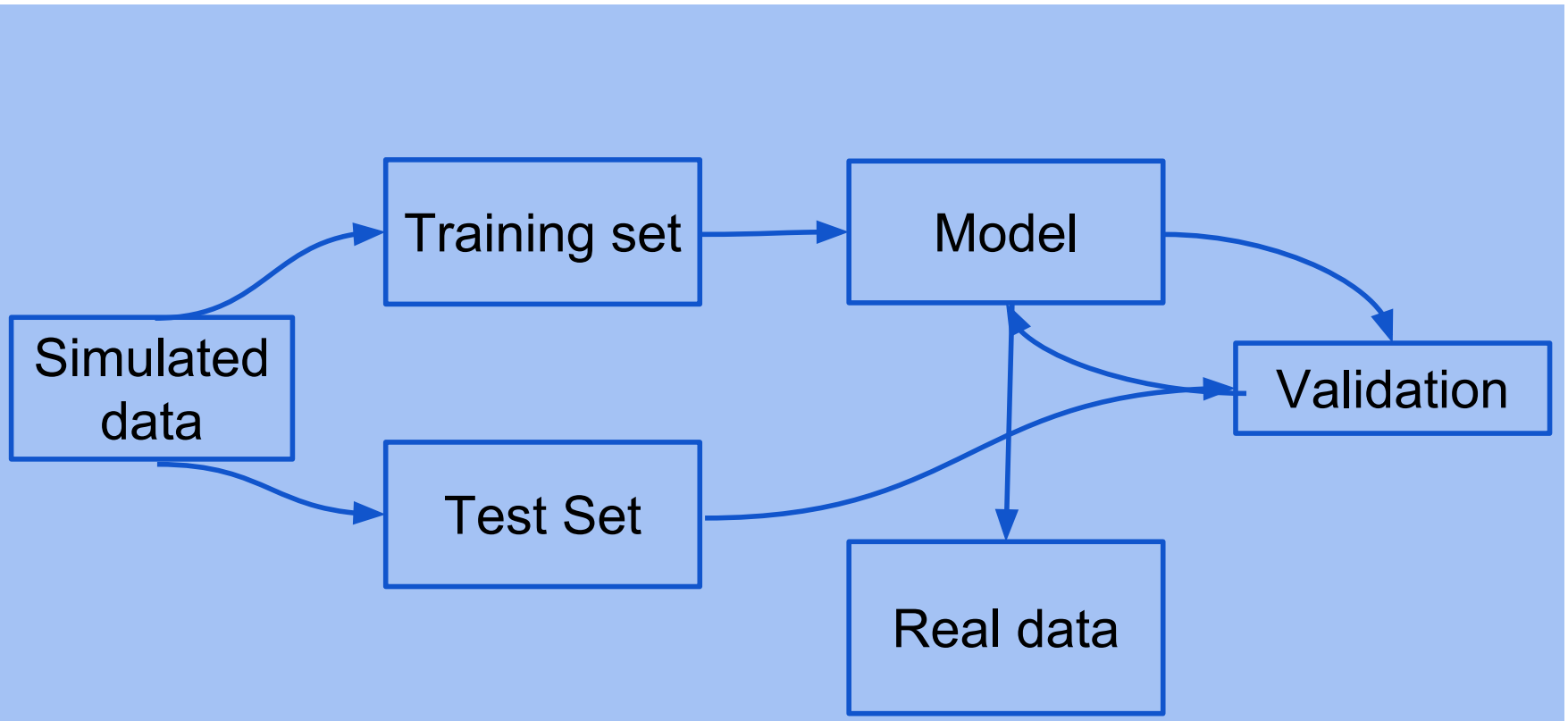

Random Forest

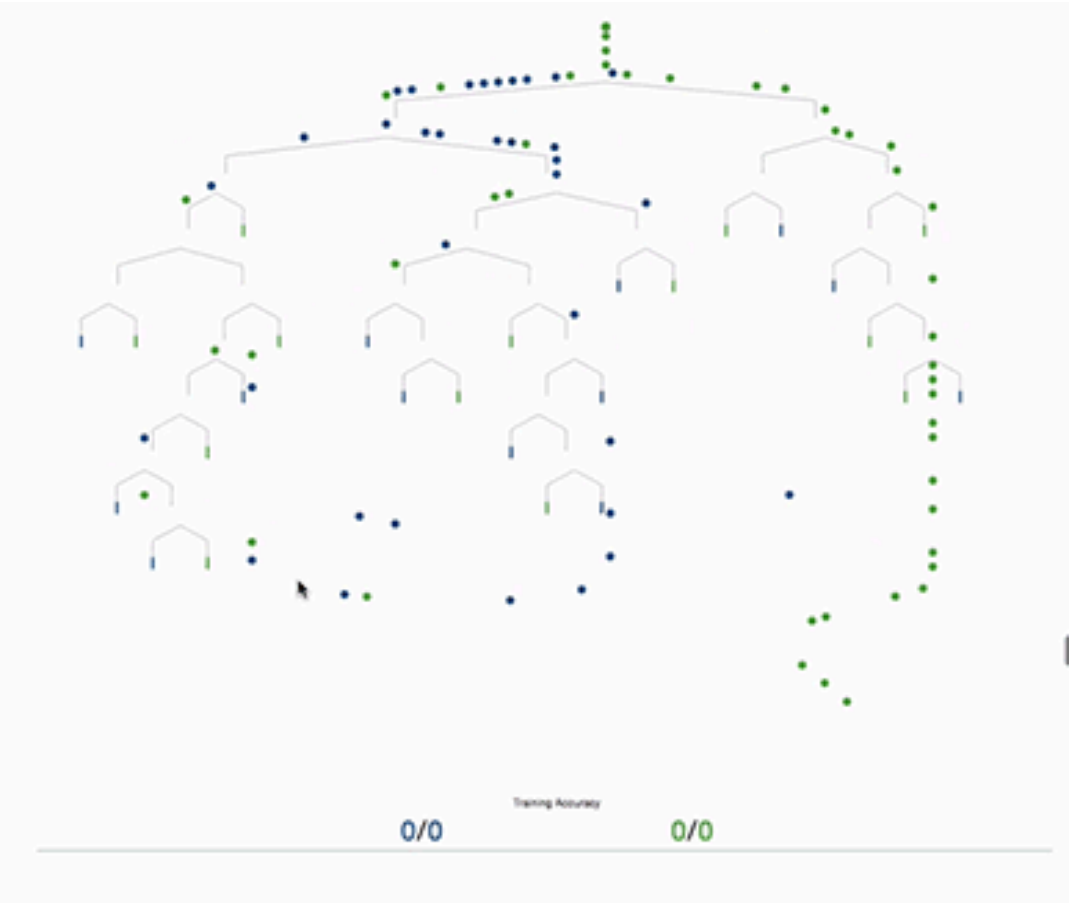

Support Vector Machines

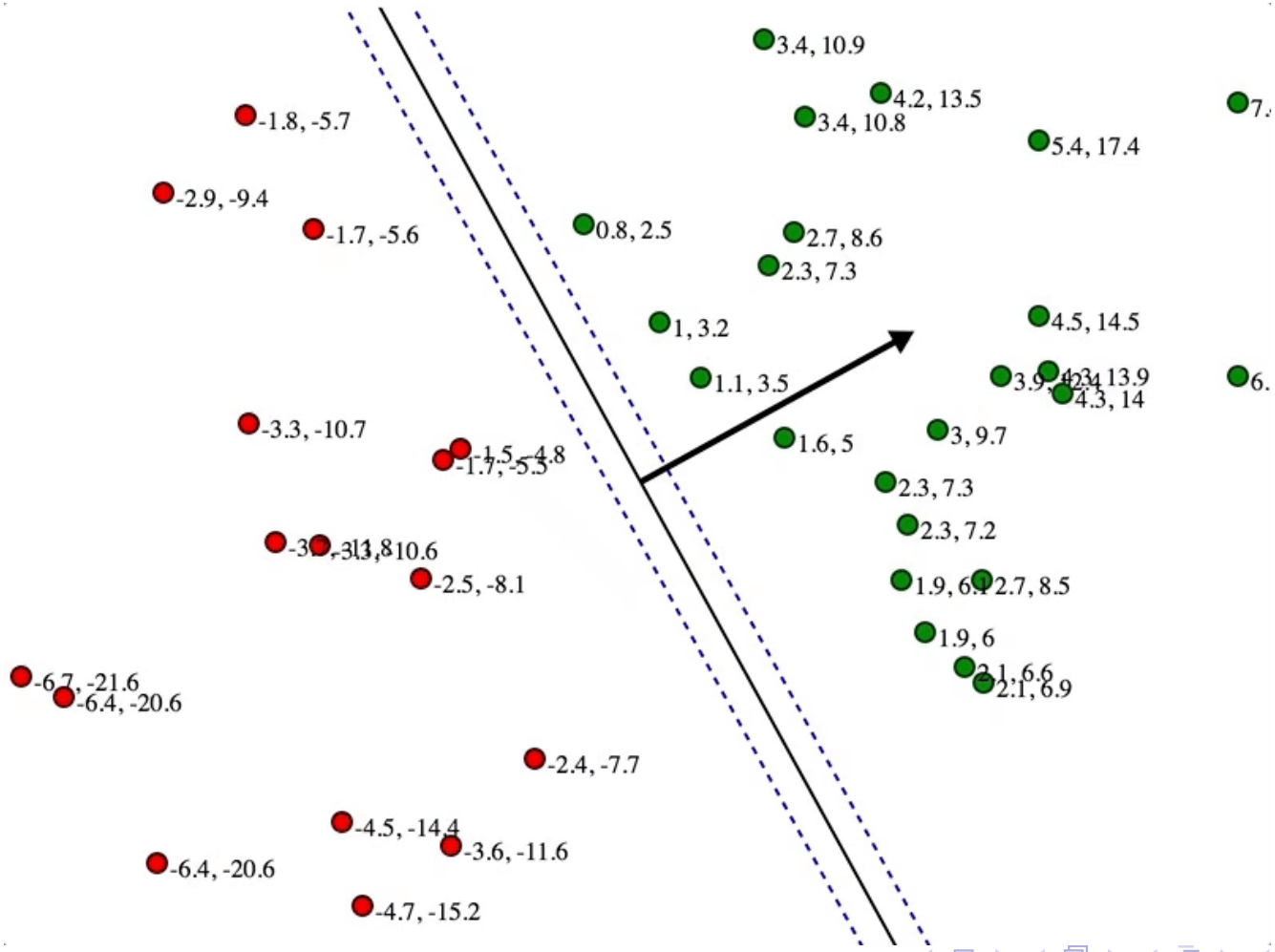

Unsupervised Learning.

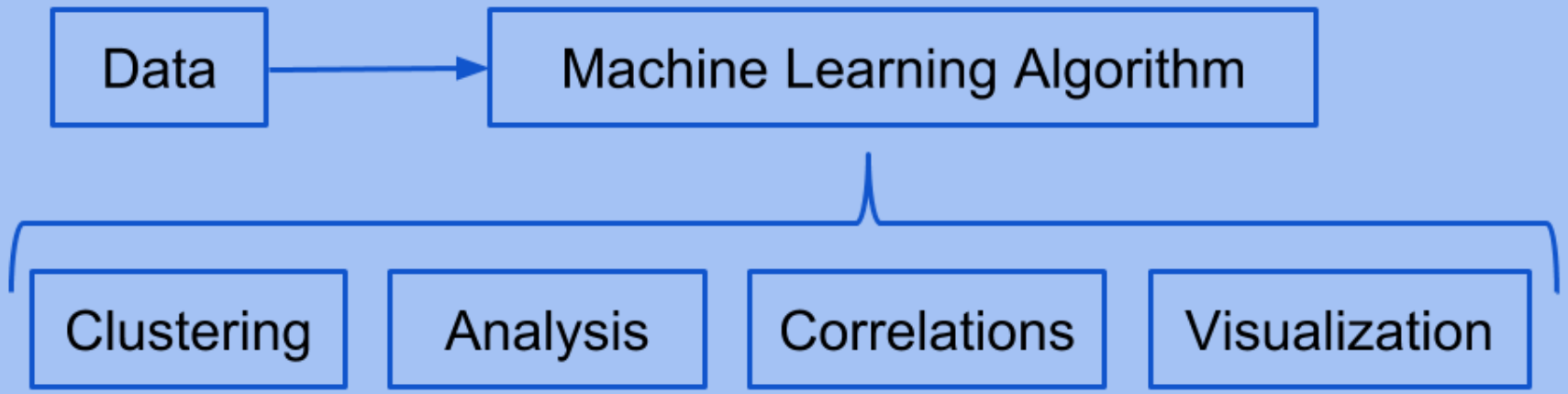

Mixture of Gaussians

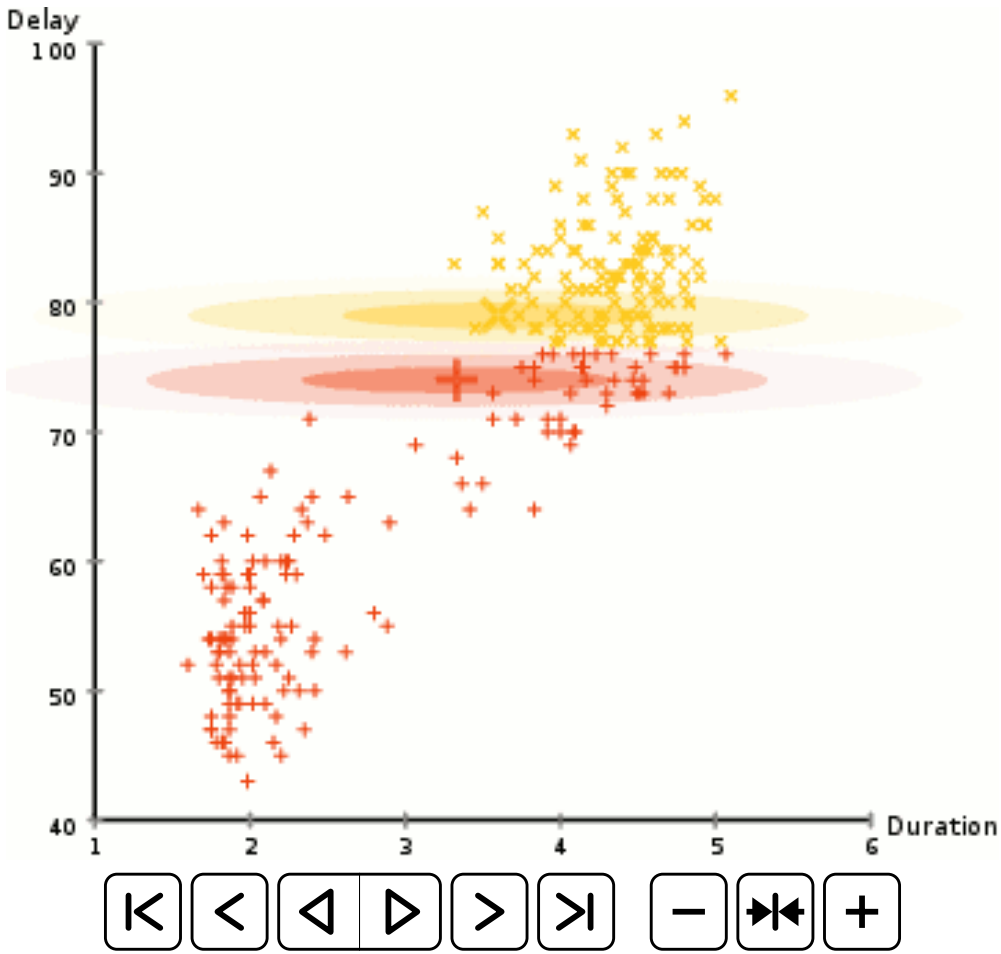

Principal Components Analysis.

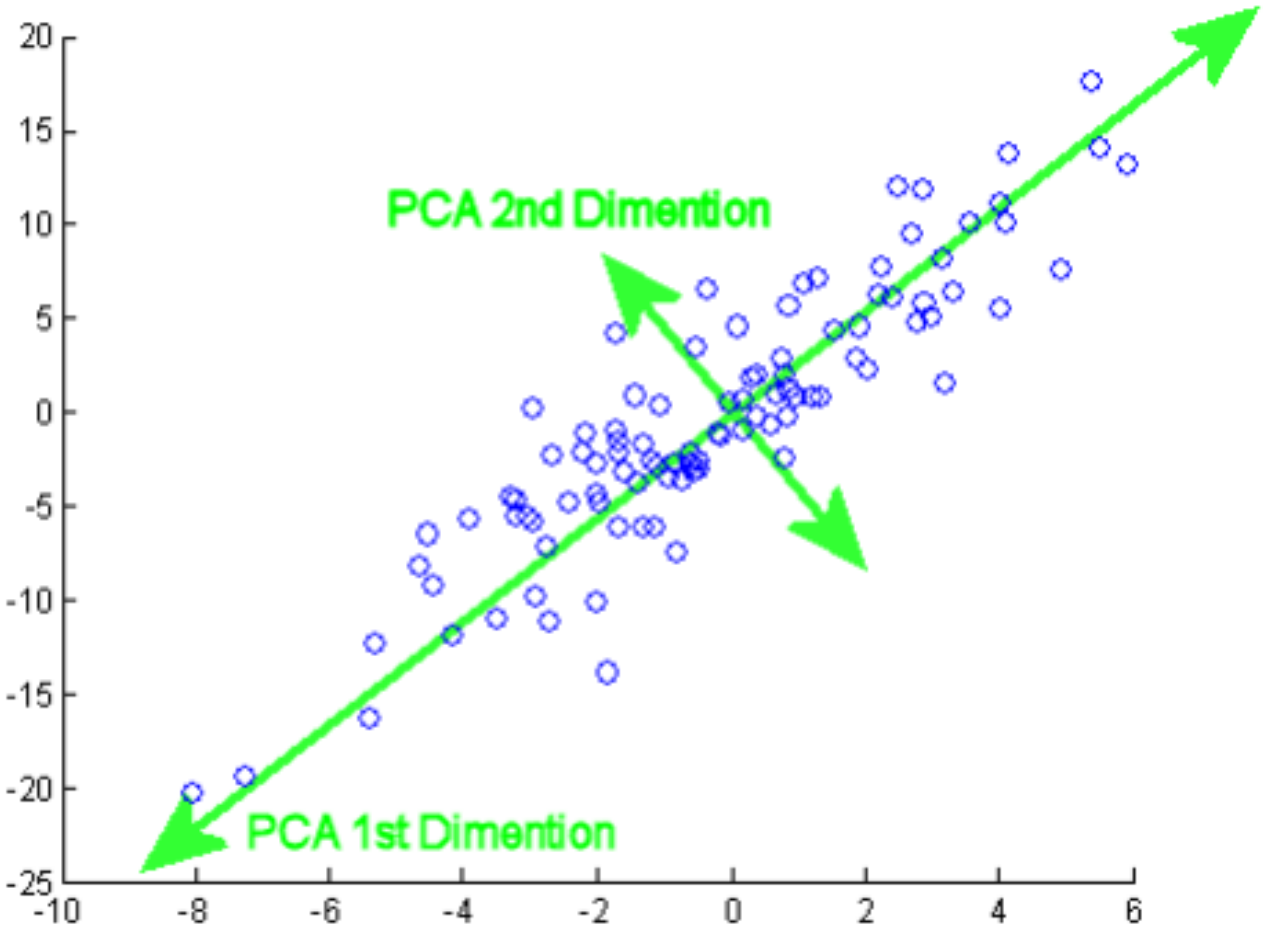

The MeSsI (Merging Systems Identification) Algorithm & Catalogue.

Martín de los Rios[⋆] Mariano J. Domínguez R.[⋆] Dante Paz, Manuel Merchán [1,2,3].
[1] *Instituto de Astronomía Teórica y Experimental (IATE-CONICET-UNC), Laprida 854, X5000BGR, Córdoba, Argentina.*
[2] *Observatorio Astronómico de Córdoba, Universidad Nacional de Córdoba, Laprida 854, X5000BGR, Córdoba, Argentina.*
[3] *Consejo Nacional de Investigaciones Científicas y Técnicas, Rivadavia 1917, C1033AAJ Buenos Aires, Argentina.*

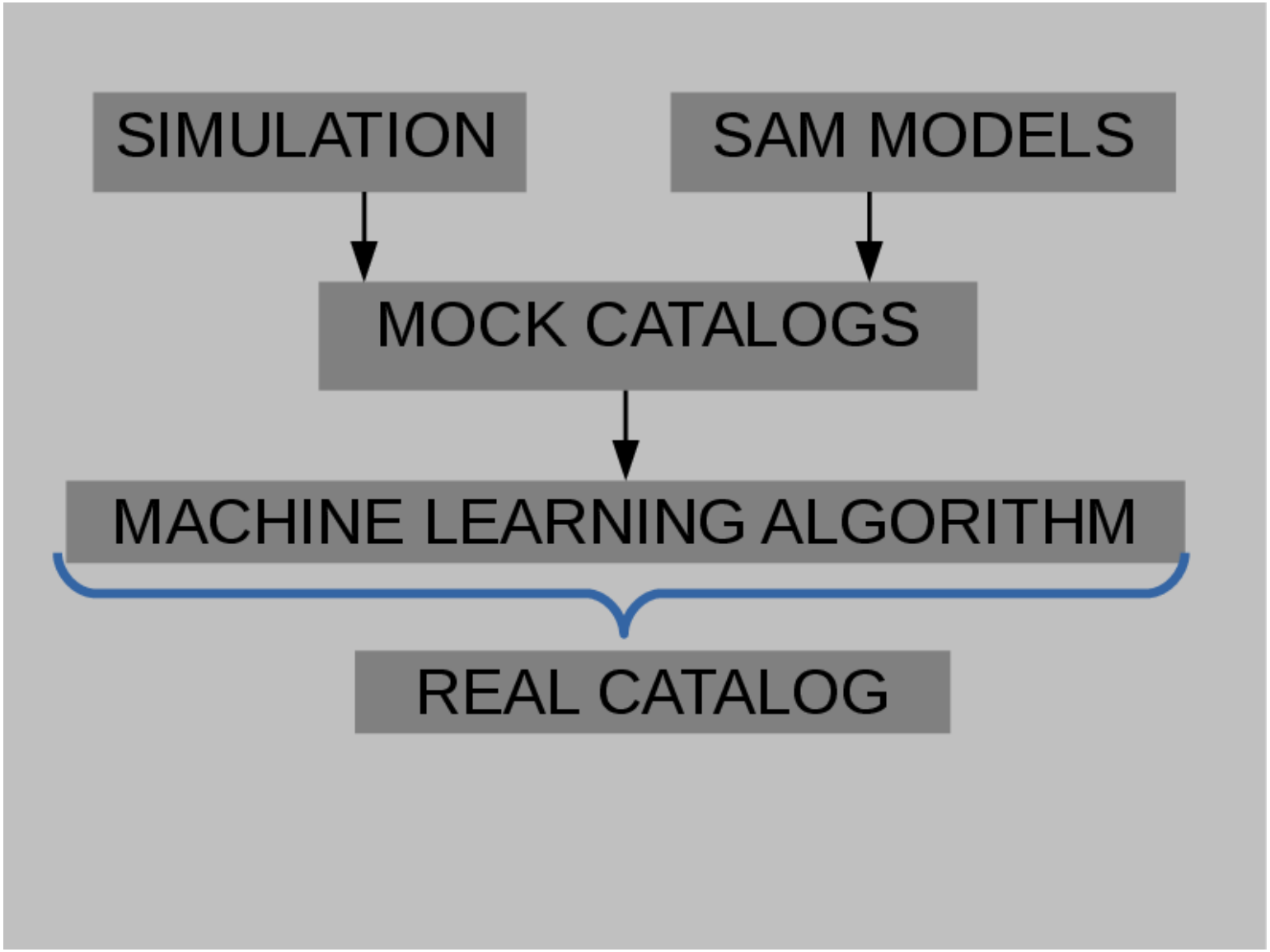
SIMULATION
SAM MODELS
MOCK CATALOGS
MACHINE LEARNING ALGORITHM
REAL CATALOG

Study of the merger trees.

- Based on the subhalos merger trees, we construct the merger tree for every fof group in the simulation.

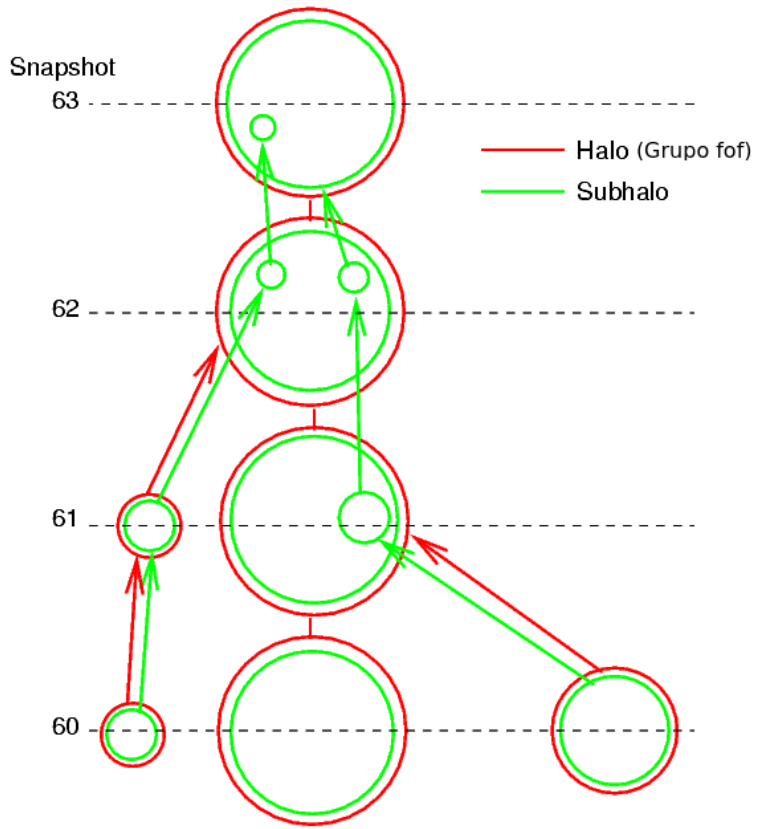

- Dressler-Shectman test.
- Non gaussianity test.
- Color.
- Number of galaxies.

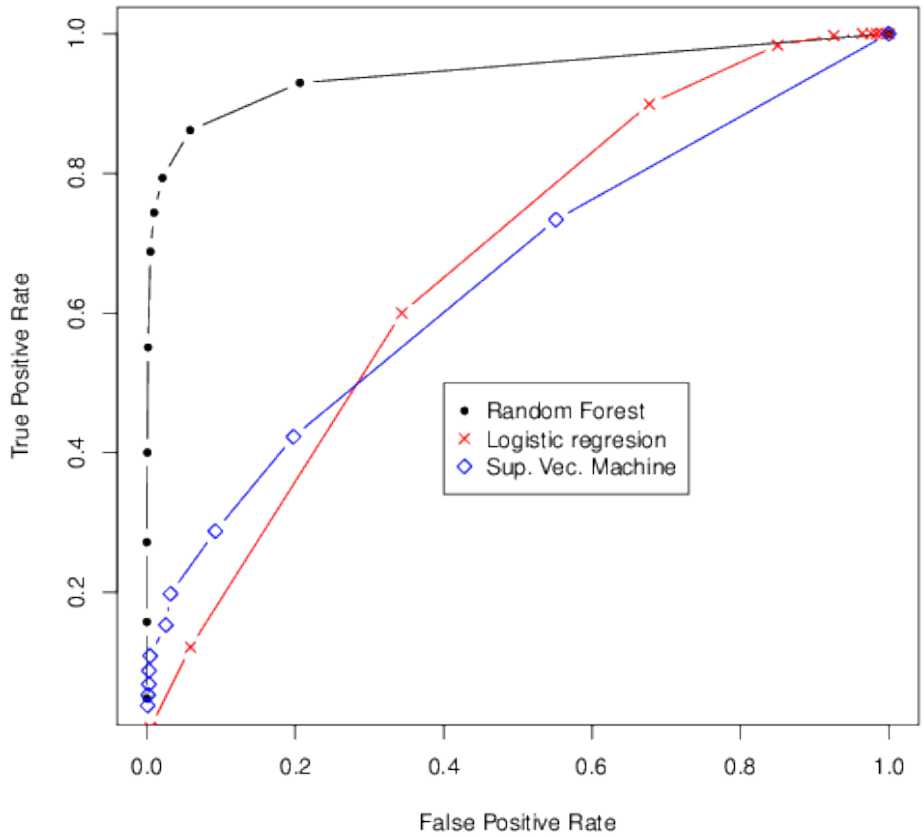

- We found 61 candidates to merging clusters.
- In 32 of these we were able to identify the colliding substructures.
- 21 of these were previously classified as merging clusters by other authors.

Name	M_1 $[10^{14} M_\odot]$	RA_1[°]	DEC_1 [°]	z_1	M_2 $[10^{14} M_\odot]$	RA_2[°]	DEC_2[°]	z_2
Abell 1991	5.7	223.58	18.53	0.0583	2.6	223.67	18.67	0.0586
	±1.2	±0.05	±0.09	±0.0003	±1.02	±0.6	±0.1	±0.0003
Abell 1424	4.9	179.38	5.08	0.0760	5.1	179.19	5.01	0.0746
	±2.3	±0.09	±0.02	±0.0004	±1.4	±0.1	±0.04	±0.0005
Abell 1589	5.5	190.25	18.53	0.0721	1.1	190.34	18.22	0.0716
✓	±0.4	±0.01	±0.02	±0.0001	±0.5	±0.01	±0.005	±0.0002
31170	25.4	255.63	34.06	0.0993	13.3	255.76	33.90	0.0989
	±0.8	±0.05	±0.05	±0.0001	±1.3	±0.005	±0.005	±0.0002
Abell 2029/33	24.3	227.73	5.68	0.0796	13.4	227.81	6.13	0.0805
	±4.6	±0.05	±0.1	±0.0004	±1.8	±0.1	±0.2	±0.0009
Abell 2069	22.6	230.99	29.94	0.1146	32	231.07	29.86	0.1146
✓	±6.8	±0.05	±0.04	±0.0002	±10	±0.05	±0.09	±0.0004
Abell 2142	18.3	239.61	27.23	0.0901	11.3	239.33	27.5	0.0893
✓	±0.6	±0.005	±0.005	±0.0004	±1.8	±0.005	±0.005	±0.0001
Abell 1913	5.5	216.73	16.75	0.0530	2.1	216.84	16.62	0.0533
	±1.1	±0.02	±0.06	±0.0004	±1.4	±0.04	±0.1	±0.0013
Abell 2399	5.1	329.29	−7.81	0.0576	2.4	329.49	−7.79	0.0581
	±0.3	±0.02	±0.02	±0.0001	±0.3	±0.04	±0.02	±0.0002
Abell 85	7.4	10.425	−9.25	0.0559	1.8	10.47	−9.51	0.0573
✓	±0.3	±0.005	±0.01	±0.0001	±1.1	±0.01	±0.05	±0.002
55731	1.9	244.72	24.21	0.0661	2.05	244.63	24.32	0.0656
	±0.4	±0.06	±0.08	±0.0004	±0.3	±0.07	±0.08	±0.0005
Abell 1750	8.7	202.80	−1.89	0.0868	7.5	202.82	−1.73	0.0848
✓	±1.1	±0.02	±0.02	±0.0009	±1.6	±0.04	±0.1	±0.0016
Abell 3158	37.24	55.75	−53.63	0.0633	4.6	55.37	−53.48	0.0622
✓	±1.5	±0.07	±0.004	±0.0001	±0.2	±0.007	±0.001	±0.0001
Abell 376	19.7	41.46	36.89	0.0478	4.01	41.72	36.94	0.0489
	±1.4	±0.006	±0.005	±0.0001	±1.09	±0.003	±0.007	±0.0002
Abell 3490	44.76	176.42	−34.37	0.0688	116.5	176.1	−34.39	0.0727
	±4.3	±0.02	±0.01	±0.0001	±40.4	±0.1	±0.1	±0.001
Abell 2382	77.7	327.90	−15.66	0.0676	6.12	328.167	−15.62	0.0642

I. Analysis of candidates for interacting galaxy clusters

A1204 and A2029/A2033

Elizabeth Johana Gonzalez[1,2], Martín de los Rios[1,2], Gabriel A. Oio[1,2], Daniel Hernández Lang[3], Tania Paez Tagliaferro[3,4], Mariano J. Domínguez R.[1,2], José Luis Nilo Castellón[3,4], Héctor Cuevas L.[3], and Carlos A. Valotto[1,2]

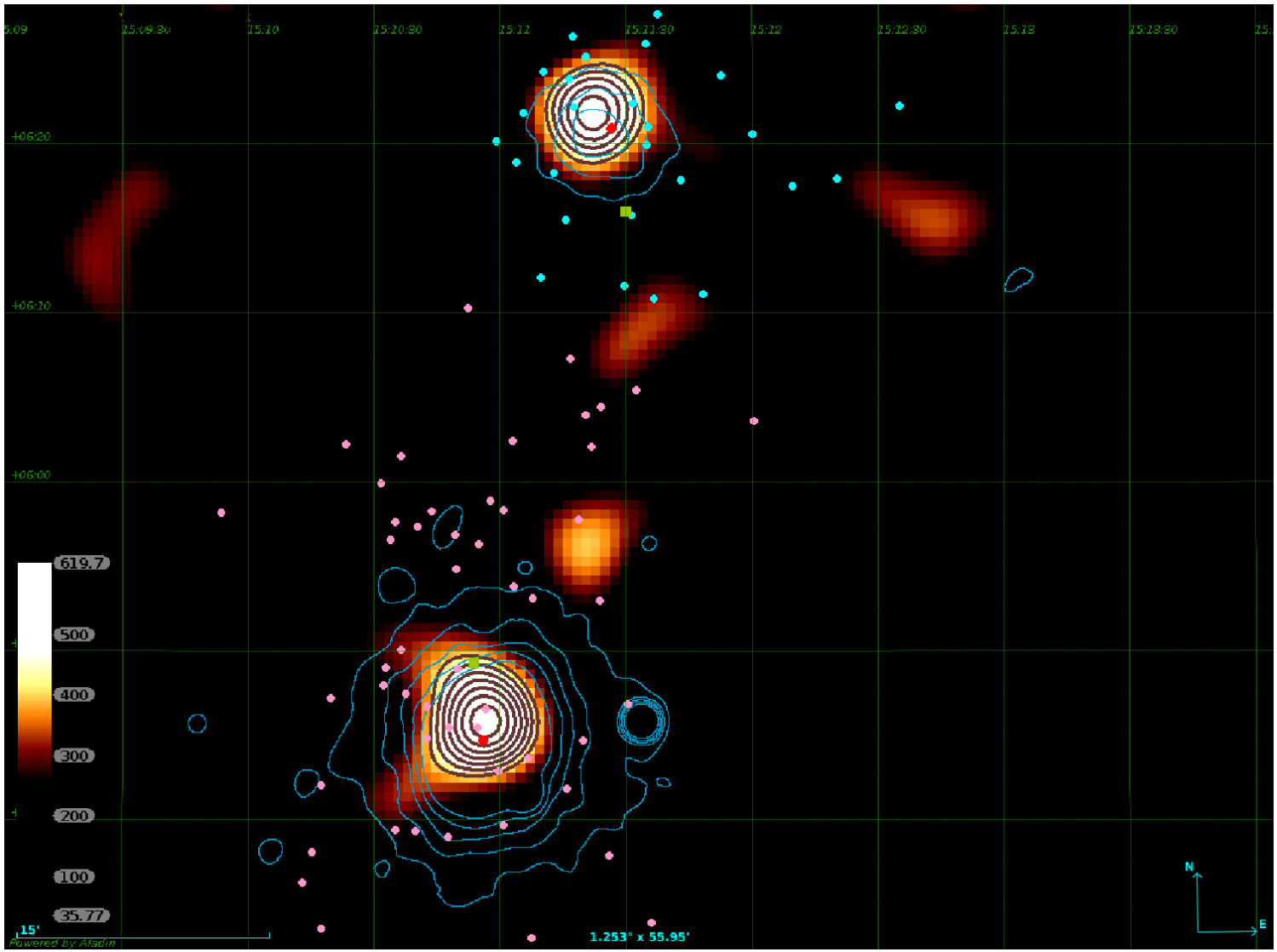
15:09:30
15:10
15:10:30
15:11
15:11:30
15:12
15:12:30
15:13
15:13:30
+06:20
+06:10
+06:00
619.7
500
400
300
200
100
35.77
15'
Powered by Aladin
1.253° x 55.95'
N
E

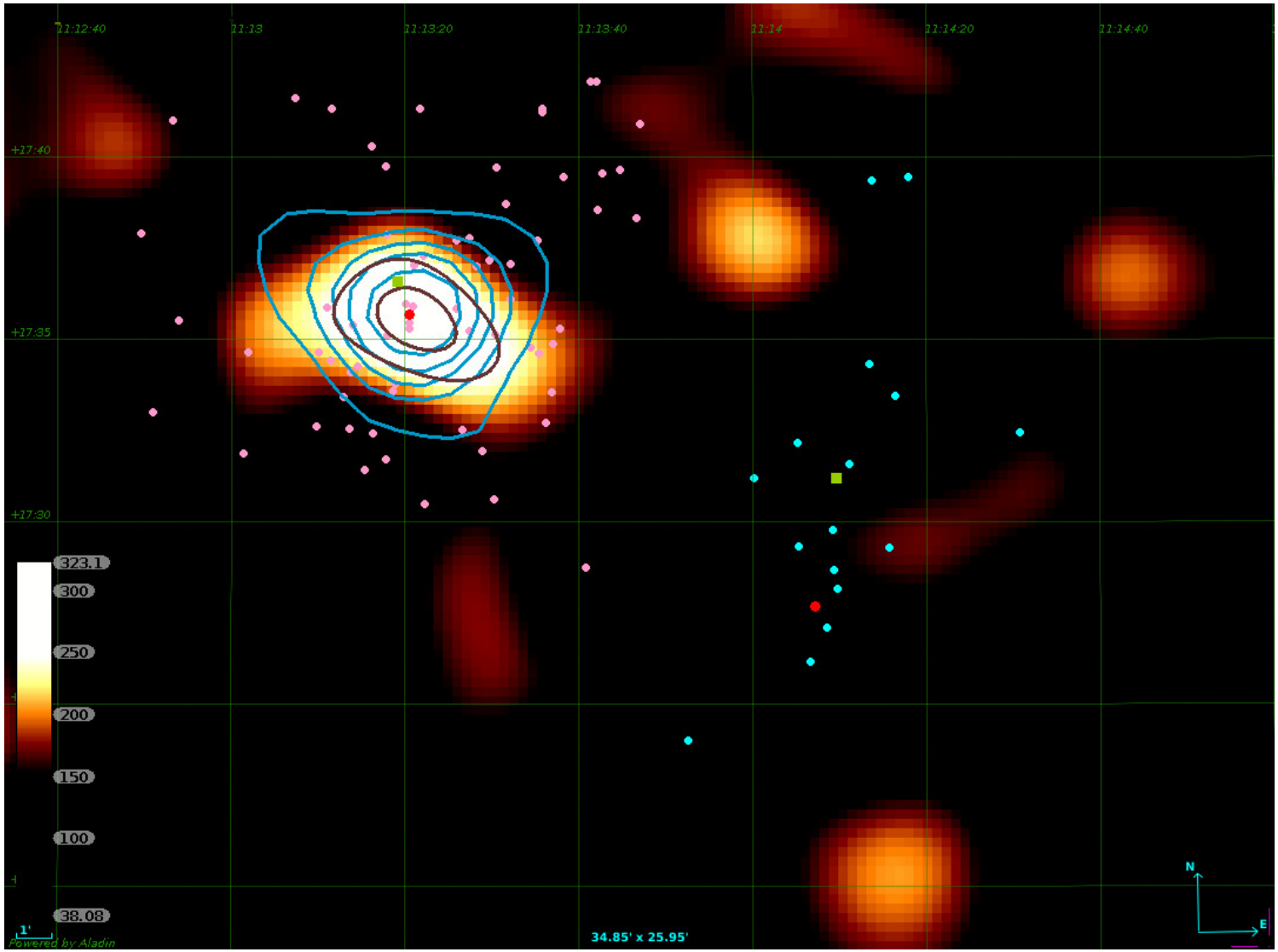
11:12:40
11:13
11:13:20
11:13:40
11:14
11:14:20
11:14:40
+17:40
+17:35
+17:30
323.1
300
250
200
150
100
38.03
1'
Powered by Aladin
34.85' x 25.95'
N
E

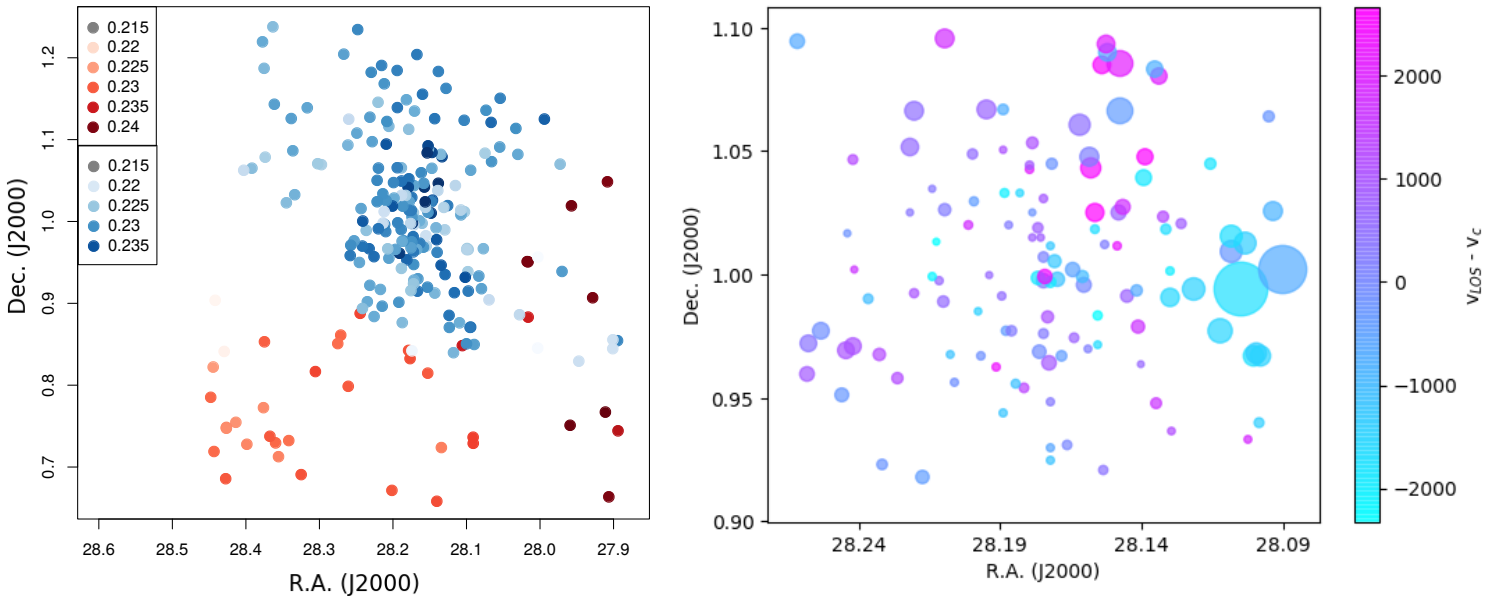
0.215
0.22
0.225
0.23
0.235
0.24
0.215
0.22
0.225
0.23
0.235
Dec. (J2000)
R.A. (J2000)
28.6
28.5
28.4
28.3
28.2
28.1
28.0
27.9
0.7
0.8
0.9
1.0
1.1
1.2
1.10
1.05
1.00
0.95
0.90
28.24
28.19
28.14
28.09
2000
1000
0
−1000
−2000
v_{LOS} - v_c

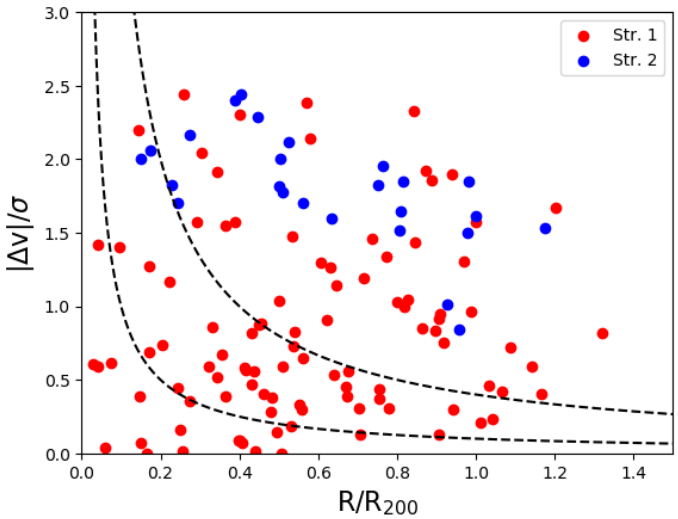
Str. 1
Str. 2
|Δv|/σ
R/R200
0.0
0.5
1.0
1.5
2.0
2.5
3.0
0.2
0.4
0.6
0.8
1.2
1.4

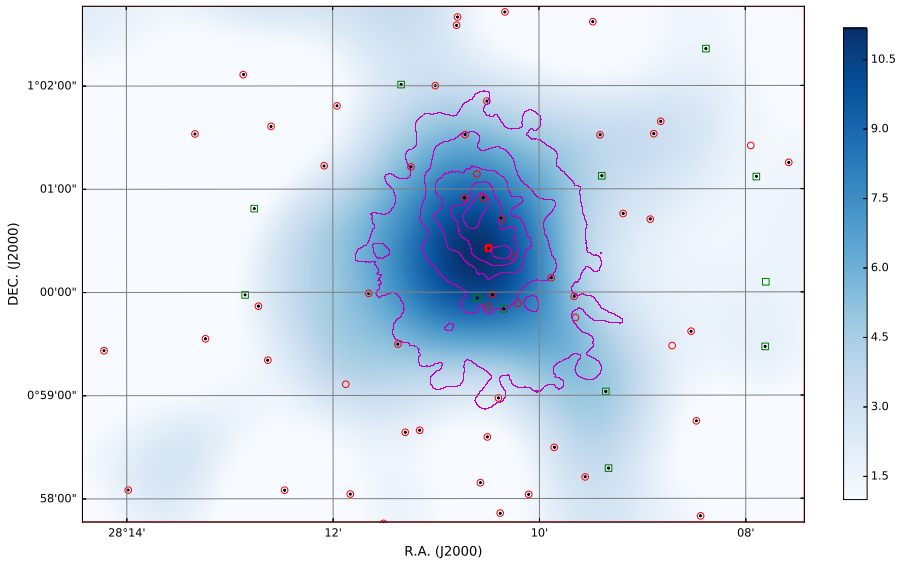
1°02'00"
01'00"
00'00"
0°59'00"
58'00"
DEC. (J2000)
28°14'
12'
10'
08'
R.A. (J2000)
10.5
9.0
7.5
6.0
4.5
3.0
1.5

MNRAS **000**, 000–000 (0000) Preprint March 8, 2019 Compiled using MNRAS LATEX style file v3.0

Faraday Rotation Measure dependence with galaxy clusters dynamics

F.A. Stasyszyn[1,2] & M. de los Rios[1,2,3]
[1] *Instituto de Astrofísica Teórica y Experimental (IATE), Laprida 854, Córdoba, Argentina*
[2] *Observatorio Astronómico de Córdoba, Universidad Nacional de Córdoba, Laprida 854, X5000BGR, Córdoba, Argentina.*
[3] *Consejo Nacional de Investigaciones Científicas y Técnicas, Rivadavia 1917, C1033AAJ Buenos Aires, Argentina.*

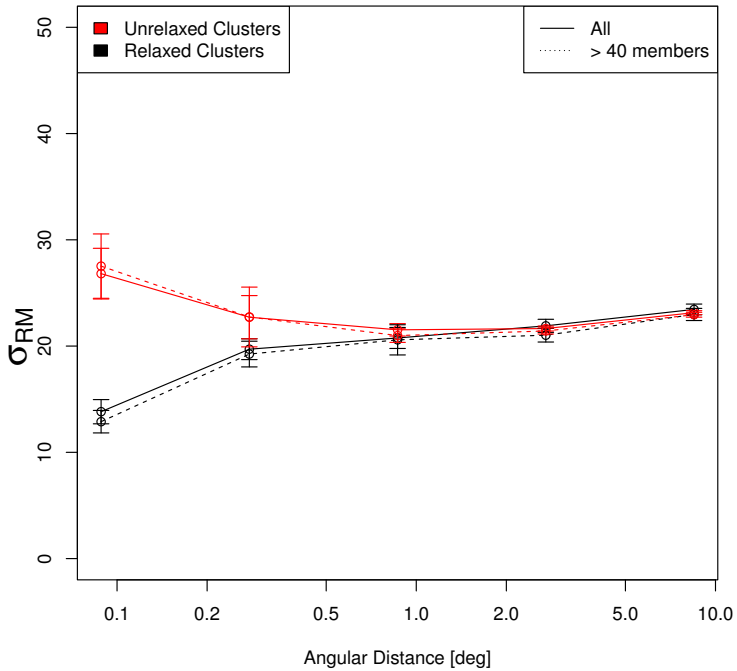
Unrelaxed Clusters
Relaxed Clusters
All
> 40 members
σRM
0
10
20
30
40
50
0.1
0.2
0.5
1.0
2.0
5.0
10.0
Angular Distance [deg]

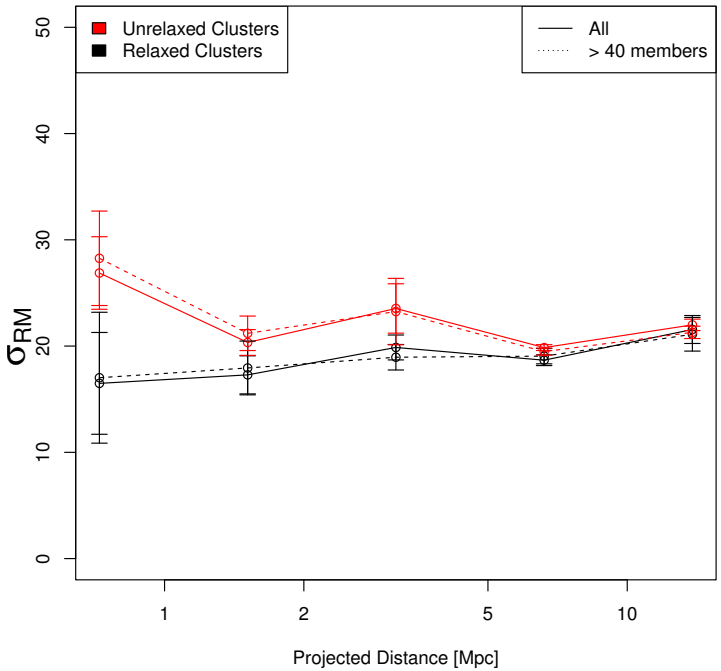
Unrelaxed Clusters
Relaxed Clusters
All
> 40 members
σRM
0
10
20
30
40
50
1
2
5
10
Projected Distance [Mpc]


Muchas
Gracias